PHYSICAL REVIEW D VOLUME 42, NUMBER 3 1 AUGUST 1990

Probing gluon and charm densities using W and Z hadroproduction at large p_T

C. S. Kim, A. D. Martin, and W. J. Stirling
Department of Physics, University of Durham, Durham, DH1 3LE, England
(Received 18 May 1990)

We show that the associated production of a W boson and a charm quark in high-energy pp or $p\bar{p}$ collisions provides a measure of the gluon distribution (at $x \sim M_W/\sqrt{s}$). Comparison with associated Zc production gives a determination of the ratio of the charm- to the strange-quark density distributions.

The recent improvement in the data for deep-inelastic lepton-nucleus scattering and for the Drell-Yan process allows a much more definitive determination of the quark distribution functions of the nucleon than hitherto managed.[1] However, the gluon distribution $G(x,Q^2)$ is not well constrained by these processes, since it only enters as a second-order effect. On the other hand, the gluon contributes to lowest order for prompt-photon production, and it has become normal practice[1,2] to use fixed-target $pp \to \gamma X$ data to determine the gluon distribution for $x \sim 2p_T/\sqrt{s}$ (where p_T is the transverse momentum of the produced photon). This, together with the momentum sum rule, is sufficient to determine the two-parameter form

$$xG(x,Q^2)=A(1-x)^{\eta}.$$

Even with a rather freely parametrized gluon, a phenomenological analysis[3] has shown that these constraints are sufficient to determine the gluon distribution to within $\pm 25\%$ for $x \gtrsim 0.02$, where the error decreases as Q^2 increases. Of course, if we extrapolate to smaller values of x, then we find that the gluon is not so precisely known.

In principle, collider data obtained for $p\bar{p} \to \gamma X$ at the Fermilab energy ($\sqrt{s}=1.8$ TeV) with $p_T \sim 10$ GeV/c could probe the gluon at $x \sim 10^{-2}$, and prompt-photon experiments at the Superconducting Super Collider (SSC) energy ($\sqrt{s}=40$ TeV) with $p_T \sim 40$ GeV/c would reach $x \sim 2\times 10^{-3}$. However, a detailed study[4] of the uncertainties in the theoretical predictions of prompt-photon production at collider energies has shown that such determinations will be difficult. One problem is the importance of the bremsstrahlung component at small p_T, in which the photon is radiated from an outgoing quark and so occurs in the debris of a hadronic jet. At collider energies such bremsstrahlung processes ($gg \to q\bar{q}\gamma$, $gq \to gq\gamma$, etc.) are particularly significant at small $x_T \equiv 2p_T/\sqrt{s}$, as the fragmentation of a quark into a photon involves (i) a large logarithmic term and (ii) a fragmentation function which is peaked at small values of z, the fraction of the quark momentum carried by the photon. These compensate for the extra power of α_s which occurs relative to the lowest-order contribution $qg \to q\gamma$. The main uncertainty in the bremsstrahlung component is the lack of knowledge of the shape of the fragmentation function. At fixed-target energies ($\sqrt{s} \lesssim 50$ GeV), which probe higher x_T values, the bremsstrahlung component can be safely ignored since it has a much steeper x_T dependence than the leading-order term. At collider energies this component can of course be reduced by selecting only events with isolated photons, but then there is the problem of matching the experimental and theoretical isolation criteria.[4]

A second ambiguity is related to the choice of scales: the factorization scale M occurring in the structure functions and the renormalization scale μ in α_s. At fixed-target energies it is found[5] that there exist (comparable) values of M and μ for which the next-to-leading logarithmic-order prediction of the cross section is stable to changes of scale. These are known as the optimized scales. At the collider energy $\sqrt{s}=1.8$ TeV, and for $p_T \sim 20$ GeV/c, optimization is still possible with M and μ rather different (large M and small μ). As a consequence the results calculated using the optimized scales exceed the predictions using $\mu = M = p_T$, say, by about 30%.[4]

A third ambiguity is the possibility that the charm-quark distribution of the proton makes a significant contribution to $p\bar{p} \to \gamma X$ at low x_T values,[6] where the sea distribution dominates over valence. In fact, Aurenche, Baier, and Fontannaz[4] find for $\sqrt{s}=1.8$ TeV and $p_T \sim 10$ GeV/c that 10% of the cross section is due to charm if the optimized scales are used (and 15% if $\mu = M = p_T$). To separate the charm (sea) contribution from the large bremsstrahlung components ($gg \to c\bar{c}\gamma$, $gg \to b\bar{b}\gamma$) will pose even more of a problem in this case. In summary we conclude that it will be extremely difficult to probe the gluon at small x (or the charm distribution) using prompt-photon data at collider energies.

Instead of using prompt-photon production, we study here the related processes of "prompt" W,Z production as a means of probing the gluon and charm distributions. In particular, we incorporate a charm tag ($c \to \mu$) to select events which, at leading order, are mediated by the subprocesses

$$sg \to cW\,, \tag{1}$$

$$cg \to cZ\,. \tag{2}$$

To be useful these processes will have to have important advantages to compensate for the higher statistics expected for prompt-photon production. First we note that the bremsstrahlung W,Z processes are negligible. The outgoing quark will very rarely fragment into a W or Z and the cross section for $gg \to c\bar{c}(W,Z)$ can be safely ignored. Moreover there is less ambiguity associated with the choice of scales. Indeed we find that, with sufficient statis-

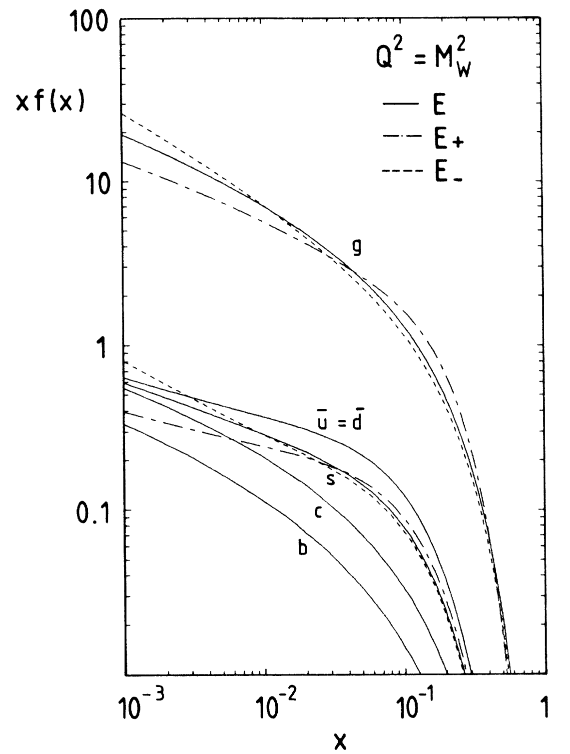

FIG. 1. The gluon and sea-quark distributions at $Q^2 = M_W^2$ of HMRS(E) (Ref. 1). For the gluon and strange sea we also show the distributions of sets E$\pm$ (Ref. 3).

tics, process (1) will offer a reliable measure of the gluon and that the ratio of (2) to (1) will provide a determination of the ratio c/s of quark densities.

To quantify these observations we calculate the p_T distribution of W and Z production at collider energies including all QCD subprocesses up to order $\alpha\alpha_s^2$.[7,8] We use the HMRS(E) parton distributions[1] which were obtained in a recent next-to-leading-order global analysis of deep-inelastic lepton-nucleus, Drell-Yan, and fixed-target prompt-photon data. To investigate the dependence on the gluon we repeat the calculation using two additional sets of parton distributions (E$\pm$) obtained in an extension[3] of the global structure function analysis in which the gluon distributions are taken to be of the form

$$xG(x,Q^2) = Ax^{\delta}(1+\gamma x)(1-x)^{\eta}, \quad (3)$$

with $\delta = \pm\frac{1}{2}$, respectively. In Fig. 1 we compare the gluon and strange-quark distributions of these three sets of parton distributions at $Q^2 = M_W^2$, as well as showing the other sea-quark distributions of set E.

The predictions for the p_T distribution of W production at $\sqrt{s} = 1.8$, 16, and 40 TeV are shown in Fig. 2, together with the component arising from the associated production of a W and a charm quark, which includes all contributions up to order $\alpha\alpha_s^2$, such as $qg \to cW$, $q\bar{q}' \to c\bar{c}W$, $gg \to c\bar{q}W$, etc. We use the results of Arnold and Reno,[7] but include a nonzero charm-quark mass, $m_c = 1.5$ GeV, in the contribution from the main subprocess $qg \to cW$:

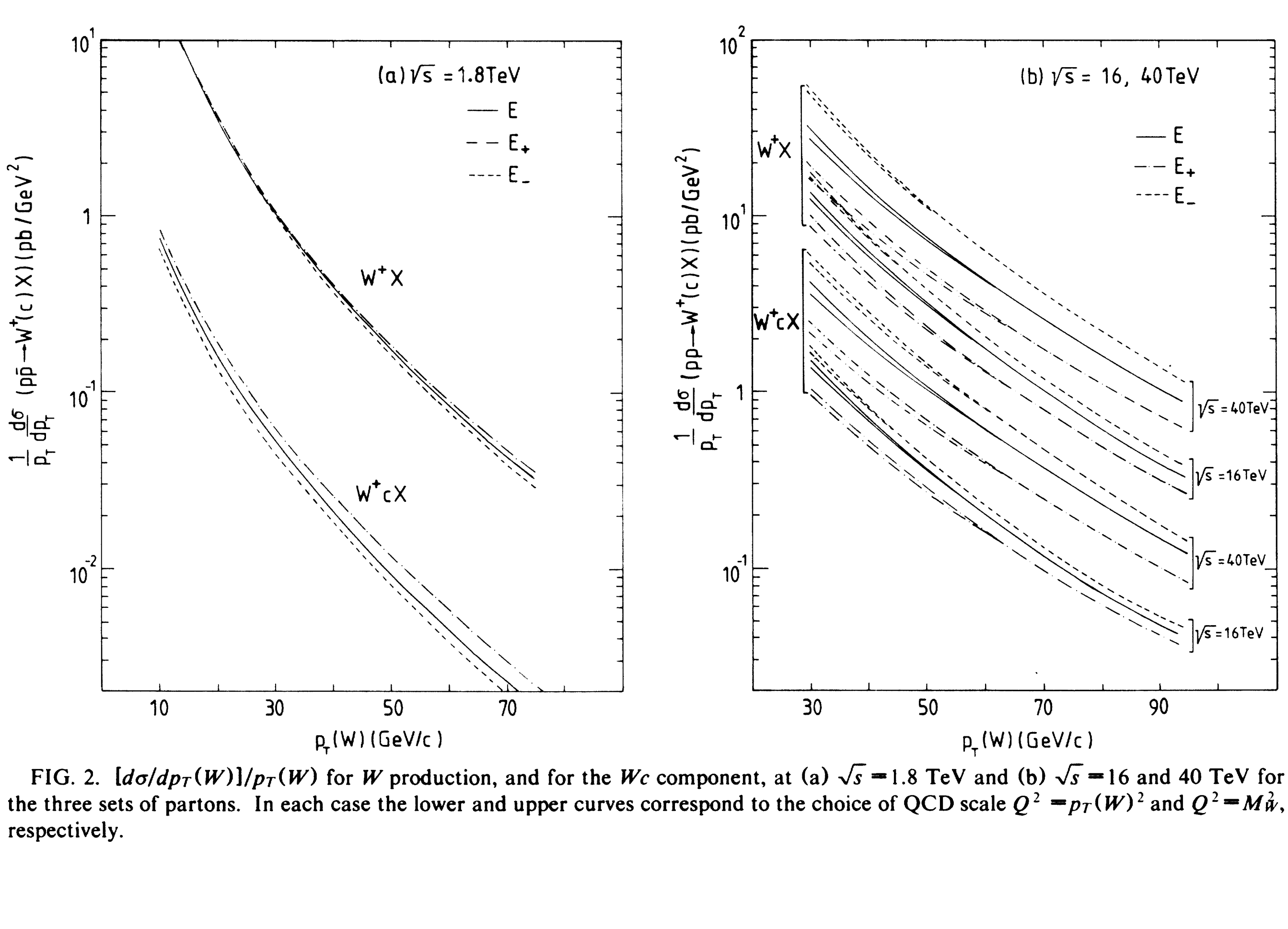

FIG. 2. $[d\sigma/dp_T(W)]/p_T(W)$ for W production, and for the Wc component, at (a) $\sqrt{s} = 1.8$ TeV and (b) $\sqrt{s} = 16$ and 40 TeV for the three sets of partons. In each case the lower and upper curves correspond to the choice of QCD scale $Q^2 = p_T(W)^2$ and $Q^2 = M_W^2$, respectively.

TABLE I. The integrated cross section for $W^{\pm}$ production, $\sigma(W)$ in nb, and for $W^{\pm}c$ associated production and decay, $\sigma(W\to e,\, c\to \mu)$ in pb, calculated using the three sets of parton distributions of Ref. 3, denoted E,E$\pm$ which have $\delta=0, \pm\frac{1}{2}$, respectively, in Eq. (3). The errors are such that the lower and upper limits correspond to the scale choice $Q^2=M_W^2$ and $Q^2=p_T(W)^2$, except that the limits are interchanged for $\sigma(W)$ at $\sqrt{s}=16$ and 40 TeV.

Structure functions	E	E+	E−
(a) Fermilab ($\sqrt{s}=1.8$ TeV), with $p_T(W)>10$ GeV/c, $p_T(\mu)>3$ GeV/c.			
$\sigma(W)$ (nb)	4.77 ± 0.09	4.83 ± 0.05	4.52 ± 0.10
$\sigma(W\to e,\, c\to\mu)$ (pb)	0.95 ± 0.03	1.11 ± 0.03	0.82 ± 0.04
(b) LHC ($\sqrt{s}=16$ TeV), with $p_T(W)>30$ GeV/c, $p_T(\mu)>10$ GeV/c.			
$\sigma(W)$ (nb)	19.0 ± 0.4	14.1 ± 0.3	22.9 ± 0.3
$\sigma(W\to e,\, c\to\mu)$ (pb)	7.9 ± 0.2	6.4 ± 0.4	8.5 ± 0.1
(c) SSC ($\sqrt{s}=40$ TeV), with $p_T(W)>30$ GeV/c, $p_T(\mu)>10$ GeV/c.			
$\sigma(W)$ (nb)	45.0 ± 1.2	29.4 ± 0.9	67.9 ± 0.9
$\sigma(W\to e,\, c\to\mu)$ (pb)	24.5 ± 1.4	16.7 ± 2.4	31.2 ± 0.3

$$s\frac{d\hat\sigma}{dt}=\frac{\pi}{3}\frac{\alpha\alpha_s}{4\sin^2\theta_W}\frac{|V_{cq}|^2}{s}\left[\left(1+\frac{m_c^2}{2M_W^2}\right)\left(\frac{-s(t-m_c^2)-2m_c^2(t-M_W^2)}{(t-m_c^2)^2}-\frac{t-m_c^2}{s}-\frac{2[M_W^2(u-m_c^2)+m_c^2(t-M_W^2)]}{s(t-m_c^2)}\right)-\frac{m_c^2}{M_W^2}\right], \tag{4}$$

where the quantity in large square brackets reduces to the usual expression $-(s^2+t^2+2uM_W^2)/st$ in the massless-quark limit. Figure 3 shows the relative size of the $O(\alpha\alpha_s^2)$ contribution for W production and for the cW component as a function of $p_T(W)$. The corrections are significant but show that the perturbative expansion is reasonable.

In Table I we give the cross sections for WX production integrated over the region $p_T(W)>p_{\rm min}^W$, and also the component $\sigma(W\to e,\, c\to\mu)$ corresponding to associated cW production and decay in which we impose the cut $p_T(\mu)>p_{\rm min}^\mu$ on the $c\to\mu$ decay, where $p_{\rm min}^\mu$ is the minimum value of $p_T(\mu)$ that can be reliably detected by experiment. The value of $p_{\rm min}^W$ is chosen so as to retain as many clean events as possible and yet to remain in a region where perturbation theory gives a reliable prediction. We take the branching ratios $B(W\to e\nu)=B(c\to\mu\nu X)=0.1$. We use a collinear approximation for the decay $c\to D(c\bar q)\to\mu\nu+$jet with a Peterson *et al.*[9] form for the fragmentation function $D_{c\to D}(z)$, and we take $D_{D\to\mu}(y)=2(1-3y^2+2y^3)$, where y and z are fractions of the appropriate parent momentum. The same scale is chosen for the parton densities and for the argument of α_s. To display the dependence on the choice of scale the errors shown in Table I are such that the limits correspond to taking $Q^2=M_W^2$ and $Q^2=p_T(W)^2$.

At the Fermilab collider energy ($\sqrt{s}=1.8$ TeV) the total W cross section is not very sensitive to the gluon density, whereas, as expected, the value of the component $\sigma(W\to e,\, c\to\mu)$ is a measure of the gluon at $x\sim0.05$. We note that to measure the gluon density at $x\sim0.05$ to an accuracy of $\pm20\%$ will require an integrated luminosity of about 25 pb^{-1}. At CERN Large Hadron Collider (LHC) and SSC energies ($\sqrt{s}=16$ and 40 TeV) the

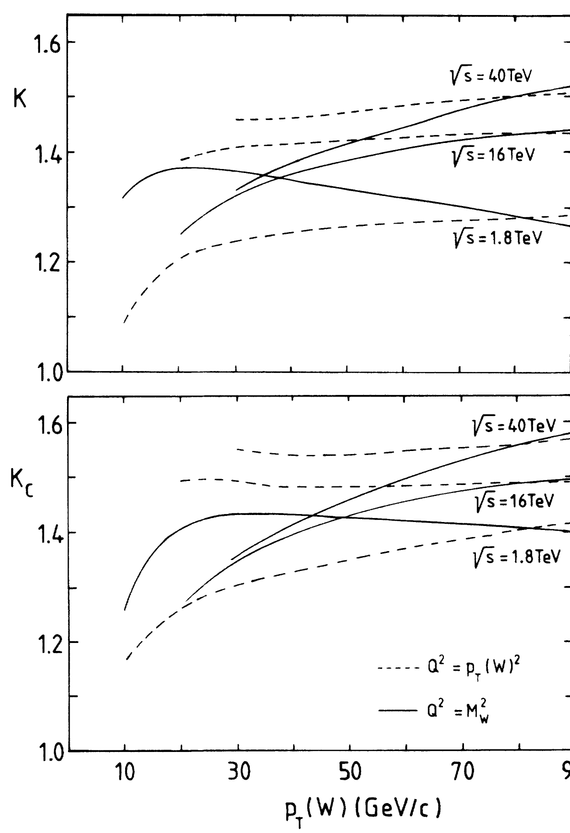

FIG. 3. $K\equiv d\sigma_3(W)/d\sigma_2(W)$ and $K_c\equiv d\sigma_3(Wc)/d\sigma_2(Wc)$ as a function of $p_T(W)$, where $d\sigma_n$ denote the differential cross sections $d\sigma/dp_T(W)$ including all QCD subprocesses up to $O(\alpha\alpha_s^n)$, using the scales $Q^2=M_W^2$ (continuous curves) and $Q^2=p_T(W)^2$ (dashed curves).

gq_{sea}-initiated processes dominate W total production [i.e., integrated over the region $p_T(W) > p_{\min}^W$], as well as the associated Wc component, and therefore they will provide a direct determination of the gluon at $x \sim 0.006$ and 0.003, respectively.

We now turn to associated Zc production with again the charm quark tagged by its decay muon. The ratio of this process to Wc production is a measure of the ratio c/s of the parton densities. Indeed, to leading order we may write

$$R_\mu \equiv \frac{\sigma(gc \to Zc) + \sigma(gb \to Zb)}{\sigma(gs \to W^\pm c)} \simeq 0.35 \left[\frac{c}{s} + 1.3 \frac{b}{s} \right] , \tag{5}$$

where we have also included the contribution from $gb \to Zb$ since it is almost impossible to tell whether the decay muon originates from charm or bottom decay (without identification of the decay vertex). To obtain an experimentally measurable ratio we must multiply R_μ of Eq. (5) by the branching-ratio factor

$$R_B \equiv \frac{B(Z \to e^+ e^-)}{B(W \to e\nu)} \simeq 0.31 , \tag{6}$$

where we have assumed $m_t \geq M_W - m_b$ and three light neutrino species.

The results for the complete calculation up to $O(\alpha\alpha_s^2)$ and including quark mixing effects are shown in Table II. We use the HMRS(E) parton distributions[1] and give results for two choices of the QCD scale. We list the values of the observable ratio $R_\mu R_B$ both with and without the contribution from associated Zb production. The ratio is found to be approximately independent of the choice of the gluon, but, as seen in Table II, it is quite scale dependent, particularly for the contribution from associated Zb production. The scale dependence is a reflection of the effect of the heavy-quark thresholds in the Q^2 evolution of the parton densities. The measurement of the ratio $R_\mu R_B$ will require high statistics, but will be very informative on the properties of the heavy-quark content of the proton.

TABLE II. The ratio of associated Zc to Wc production with the Z to W branching-fraction factor R_B of Eq. (6) included. The values of the ratio ($R_\mu R_B$) are shown both with and without the contribution from Zb production, for three collider energies, $\sqrt{s} = 1.8$, 16, and 40 TeV, with the cuts specified in Table I applied. The errors are such that the lower and upper limits correspond to the choice of QCD scale $Q^2 = p_T(W)^2$ and $Q^2 = M_W^2$, respectively.

$\sigma(Zc)/\sigma(Wc)$ (TeV)	Without Zb	With Zb
$\sqrt{s} = 1.8$	0.030 ± 0.003	0.050 ± 0.010
$\sqrt{s} = 16$	0.057 ± 0.001	0.106 ± 0.007
$\sqrt{s} = 40$	0.064 ± 0.002	0.123 ± 0.008

The luminosity available at the Fermilab $p\bar{p}$ collider is probably insufficient to determine $R_\mu R_B$ and it may be more useful to probe the charm distribution by measuring[10]

$$B(y) \equiv \frac{\sigma_{W^+}(y) + \sigma_{W^-}(y)}{\sigma_Z(y)} \tag{7}$$

as a function of the rapidity y. However, at the proposed LHC and SSC, with integrated luminosities of 10^4 pb^{-1} or higher, the event rate will be more than sufficient to reliably determine $R_\mu R_B$.

We would like to thank J. Collins and K. Tesima for helpful discussions. The work was supported by the United Kingdom Science and Engineering Research Council.

[1] P. N. Harriman, A. D. Martin, W. J. Stirling, and R. G. Roberts, this issue, Phys. Rev. **42**, 798 (1990).

[2] P. Aurenche, R. Baier, M. Fontannaz, J. F. Owens, and M. Werlen, Phys. Rev. D **39**, 3275 (1989).

[3] P. N. Harriman, A. D. Martin, W. J. Stirling, and R. G. Roberts, Phys. Lett. (to be published).

[4] P. Aurenche, R. Baier, and M. Fontannaz, Phys. Rev. D (to be published).

[5] P. Aurenche, R. Baier, M. Fontannaz, and D. Schiff, Nucl. Phys. **B297**, 661 (1988).

[6] R. S. Fletcher, F. Halzen, and E. Zas, Phys. Lett. B **221**, 403 (1989).

[7] P. B. Arnold and M. H. Reno, Nucl. Phys. **B319**, 37 (1989).

[8] R. Gonsalves, J. Pawlowski, and C.-F. Wai, Phys. Rev. D **40**, 2245 (1989).

[9] C. Peterson *et al.*, Phys. Rev. D **27**, 105 (1983).

[10] K. Hagiwara, F. Halzen, and C. S. Kim, Phys. Rev. D **41**, 1471 (1990).